


ORIGINAL ARTICLE

TAF1D promotes proliferation by transcriptionally activating G2/M phase-related genes in *MYCN*-amplified neuroblastoma

Xuan Zhang¹  | Shijia Zhan¹ | Xiaoxing Guan² | Yanli Zhang³ | Jie Lu¹ | Yongbo Yu¹ | Yaqiong Jin¹ | Yeran Yang¹ | Ping Chu¹ | Enyu Hong¹ | Hui Yang¹ | Huimin Ren¹ | Di Geng¹ | Yadi Wang¹ | Pingping Zhou¹ | Yongli Guo¹ | Yan Chang¹

¹Beijing Key Laboratory for Pediatric Diseases of Otolaryngology, Head and Neck Surgery, MOE Key Laboratory of Major Diseases in Children, Beijing Pediatric Research Institute, Beijing Children's Hospital, Capital Medical University, National Center for Children's Health, Beijing, China

²Department of Pathology, Beijing Children's Hospital, Capital Medical University, National Center for Children's Health, Beijing, China

³Imaging Core Facility, Technology Center for Protein Science, Tsinghua University, Beijing, China

Correspondence

Yan Chang, Beijing Key Laboratory for Pediatric Diseases of Otolaryngology, Head and Neck Surgery, MOE Key Laboratory of Major Diseases in Children, Beijing Pediatric Research Institute, Beijing Children's Hospital, Capital Medical University, National Center for Children's Health, 56 South Lishi Road, Xicheng District, Beijing 100045, China.
Email: changyan809@ccmu.edu.cn

Funding information

A grant from Beijing Hospitals Authority, Grant/Award Number: QML20211201; Beijing Natural Science Foundation, Grant/Award Number: 7212038; National Natural Science Foundation of China, Grant/Award Number: 82141118 and 82172849; R&D Program of Beijing Municipal Education Commission, Grant/Award Number: KM202210025010; Clinical Research Special Funding Fund of Wu Jieping Medical Foundation, Grant/Award Number: 320.6750.2022-03-50

Abstract

High-risk neuroblastoma (HR-NB) is an aggressive childhood cancer that responds poorly to currently available therapies and is associated with only about a 50% 5-year survival rate. *MYCN* amplification is a critical driver of these aggressive tumors, but so far there have not been any approved treatments to effectively treat HR-NB by targeting *MYCN* or its downstream effectors. Thus, the identification of novel molecular targets and therapeutic strategies to treat children diagnosed with HR-NB represents an urgent unmet medical need. Here, we conducted a targeted siRNA screening and identified TATA box-binding protein-associated factor RNA polymerase I subunit D, *TAF1D*, as a critical regulator of the cell cycle and proliferation in HR-NB cells. Analysis of three independent primary NB cohorts determined that high *TAF1D* expression correlated with *MYCN*-amplified, high-risk disease and poor clinical outcomes. *TAF1D* knockdown more robustly inhibited cell proliferation in *MYCN*-amplified NB cells compared with *MYCN*-non-amplified NB cells, as well as suppressed colony formation and inhibited tumor growth in a xenograft mouse model of *MYCN*-amplified NB. RNA-seq analysis revealed that *TAF1D* knockdown downregulates the expression of genes associated with the G2/M transition, including the master cell-cycle regulator, cell-cycle-dependent kinase 1 (*CDK1*), resulting in cell-cycle arrest at G2/M. Our findings demonstrate that *TAF1D* is a key oncogenic regulator of *MYCN*-amplified HR-NB and suggest that therapeutic targeting of *TAF1D* may be a viable strategy to treat HR-NB patients by blocking cell-cycle progression and the proliferation of tumor cells.

Abbreviations: CDK1, cyclin-dependent kinase 1; HR-NB, High-risk neuroblastoma; INSS, International Neuroblastoma Staging System; KEGG, Kyoto Encyclopedia of Genes and Genomes.; NB, Neuroblastoma; RTCA, real-time cell analysis; TAF, TATA-box-binding protein-associated factor; *TAF1D*, TATA box-binding protein-associated factor RNA polymerase I subunit D.

Xuan Zhang and Shijia Zhan contributed equally to this study.

This is an open access article under the terms of the [Creative Commons Attribution-NonCommercial-NoDerivs](https://creativecommons.org/licenses/by-nc-nd/4.0/) License, which permits use and distribution in any medium, provided the original work is properly cited, the use is non-commercial and no modifications or adaptations are made.

© 2023 The Authors. *Cancer Science* published by John Wiley & Sons Australia, Ltd on behalf of Japanese Cancer Association.

KEYWORDS

CDK1, cell cycle progression, neuroblastoma, proliferation, TAF1D

1 | INTRODUCTION

Neuroblastoma is the most common extracranial malignant solid tumor in children, accounting for ~7% of childhood malignancies and 15% of all childhood cancer deaths.¹ NB derives from the malignant transformation of neural crest cells or chromaffin cells during development.² Based on clinical and molecular indicators, NB is stratified into low risk, intermediate risk, or high risk.³ Among HR-NB, ~40% harbor amplification of the MYCN oncogene, and a direct role for this lesion in the refractory tumor phenotype has been validated.⁴⁻⁶ Despite advances in multimodal therapy strategies that can include chemotherapy, surgery, autologous transplant, and immunotherapy, patients with HR-NB have only a 40% likelihood of 5-year overall survival.^{4,7-9} Therefore, the identification of novel molecular targets and therapeutics to treat HR-NB is urgently needed.

Uncontrolled tumor cell proliferation is a hallmark of cancer, and it is usually driven by the aberrant expression or activation of cell-cycle regulators.¹⁰ Indeed, intervening in the cell cycle was among the earliest concepts for targeted therapies in oncology, and new strategies to target cell-cycle regulators are still being pursued.¹¹ Recently, CDK inhibitors have been tested in the treatment of NB.¹² However, redundancy in cell-cycle-related genes enables adaptive reprogramming to overcome the inhibition of individual cell-cycle regulators,^{13,14} and there is an effort in the field to identify therapeutic approaches that will more broadly quench cell-cycle signaling pathways.

TAF1D is a component of the transcription factor SL1/TIF-IB complex.¹⁵ The SL1/TIF-IB complex is involved in the assembly of the pre-initiation complex and stabilizes binding factor at the rDNA promoter during RNA polymerase I-dependent transcription,^{15,16} but the specific role of TAF1D in these processes is not well understood. One insight came from a proteomics study that analyzed the phosphorylation status of all TAFs throughout the cell cycle and detected G2/M-specific phosphorylation of TAF1D,¹⁷ suggesting that TAF1D may have a role in cell-cycle regulation.

Although it has been reported that *TAF1D* is highly expressed in HR-NB,¹⁸ it remains unknown whether TAF1D has a biological function in NB pathogenesis. In this study, we prioritized genes that are highly expressed in MYCN-amplified HR-NB and that negatively correlate with survival in patients with NB and tested whether they were essential to sustain HR-NB cells. With a siRNA screening, we describe for the first time the role and mechanisms of TAF1D in NB carcinogenesis. *TAF1D* expression level negatively correlated with overall survival in three independent primary neuroblastoma cohort datasets. Moreover, silencing of *TAF1D* inhibits the growth of NB cells in vivo and in vitro, especially in MYCN-amplified HR-NB. Mechanistically, we demonstrated that *TAF1D* knockdown

downregulates the expression of G2/M phase-related genes, including the master cell-cycle kinase, CDK1, and leads to G2/M arrest. Thus, our work describes a novel cell-cycle regulatory function of TAF1D in MYCN-amplified HR-NB that warrants further investigation as a potential therapeutic target and biomarker for HR-NB.

2 | MATERIALS AND METHODS

2.1 | Antibodies and reagents

Antibodies and reagents are listed in [Tables S1](#) and [S2](#).

2.2 | Cell lines and cell culture

MYCN-amplified NB cell lines SK-N-BE(2) and IMR32 (#CRL-2271 and #CRL-127), MYCN-non-amplified NB cell lines SH-SY5Y and SK-N-SH (#CRL-2266 and #HTB-11) and lentiviral packaging cell line 293T (#CRL-3216) were from the ATCC. SK-N-BE(2) was grown in DMEM with 10% FBS, 100U/mL penicillin, and 0.1 mg/mL streptomycin. IMR32 was grown in Eagle's Minimum Essential Medium with 10% FBS, 100U/mL penicillin, and 0.1 mg/mL streptomycin. All cells were cultured in a 5% CO₂ humidified incubator at 37°C.

2.3 | Cell transfection and RNA interference

The sequences of siRNA targeting specific genes are listed in [Table S3](#). siRNA oligonucleotides were synthesized by the RiboBio Company, Guangzhou, China. For siRNA screening experiments, siRNAs were used at a final concentration of 60nM and transfected with Lipofectamine RNAiMAX transfection reagent according to the manufacturer's protocol. Cells were harvested for RNA isolation and immunoblot 72h after siRNA transfection.

2.4 | Construction of stable *TAF1D* knockdown of MYCN-amplified NB cell lines

The sequences of two shRNAs specifically targeting *TAF1D* are the same as two siRNAs for *TAF1D* (*siTAF1D-1#*, *siTAF1D-3#*). Two shRNA sequences named "shTAF1D-926#" and "shTAF1D-927#" were cloned into the lentiviral transfer plasmid (pGV654#, Shanghai Genechem Company, China) separately. 293T cells were transfected with lentiviral transfer plasmid, packaging plasmid and envelope plasmid (pHelper 1.0# and pHelper 2.0#, Shanghai Genechem

Company, China) using a calcium phosphate cell transfection kit (C0508#, Beyotime Company, China). The recombinant lentiviruses were harvested 96 h post-transfection. The multiplicities of infection for lentivirus infecting were 10 for SK-N-BE(2)/IMR32 cells and 20 for SH-SY5Y cells.

2.5 | MYCN-amplified NB xenograft mouse model

We obtained 6-week-old female BALB/c-nude mice from the Vital River Laboratory Animal Technology Company, Beijing, China. Mice were housed in specific pathogen-free conditions in the Department of Laboratory Animal Center at Capital Medical University.

For in vivo HR-NB cell xenografts, *TAF1D*-knockdown and control cells (5×10^6) were suspended in DMEM with 50% Matrigel and subcutaneously injected into the right dorsal flanks of blindly randomized nude mice ($n = 5$ per group). Mice were observed every 3 days and euthanized 31 days after cell inoculation. Tumors were excised and photographed, measured, and weighed. Some tumor tissues were subjected to RT-qPCR and immunohistochemical analysis.

2.6 | Cell viability and colony formation assays

The xCELLigence RTCA system was used for label-free and real-time monitoring of cell viability. NB cells were seeded into the xCELLigence system 24 h after transfection with siRNA, and each well was seeded with 5000 cells of SK-N-BE(2)/IMR32 or 10,000 cells of SH-SY5Y. Continuous monitoring of cell viability by the xCELLigence system was shown in the form of delta cell index determination.

For the colony formation assays, cells were plated in triplicate at 600 cells/well (SK-N-BE(2) and IMR32). After 14 days, cells were fixed with 4% paraformaldehyde for 15 min and stained with 0.1% crystal violet for 20 min. Colonies were photographed and counted using AlphaView software (ProteinSimple).

2.7 | Flow cytometry and cell-cycle analysis

SK-N-BE(2) cells were cultured in 6-well plates and transfected with siRNA. 72 h post-transfection, cells were trypsinized and then fixed with 70% ethanol at -20°C overnight. After centrifugation, cell pellets were digested with $100 \mu\text{g}/\text{mL}$ RNase A for 30 min at 37°C and stained using propidium iodide ($50 \mu\text{g}/\text{mL}$ in 0.2% Triton X-100) for 10 min. Subsequently, the cells were collected on a FACS Calibur flow cytometer and analyzed by FlowJo software (BD Biosciences). Over 1×10^4 cells were analyzed for each sample.

2.8 | Immunohistochemical analysis

The xenograft NB tumors were fixed overnight in 4% paraformaldehyde, dehydrated in a graded series of ethanol, and embedded in

melted paraffin wax. For the immunohistochemical analysis, $4 \mu\text{m}$ sections were first deparaffinized and rehydrated. Antigen retrieval was performed in a pressure cooker at 100°C for 3 min in 10 mM sodium citrate (pH 6.0) for anti-CDK1 treatment or in 1 mM EDTA (pH 9.0) for anti-Ki67 treatment, and endogenous peroxidase activity was blocked with 3% hydrogen peroxide for 15 min at room temperature. The slides were then incubated in 5% goat serum. Then, slides were incubated with primary antibodies at 4°C overnight in a humid environment. Tissues were washed extensively in PBS buffer containing 0.05% (v/v) Tween-20. Detection was performed using a HRP-conjugated secondary antibody followed by chromogenic detection using DAB as the substrate. The sections were counterstained with hematoxylin and dehydrated with ethanol and xylene prior to mounting.

2.9 | RNA isolation, reverse transcription, and RT-qPCR

Total RNA was isolated using TRIzol reagent and mRNAs were converted to cDNA using the PrimeScript™ RT Master Mix for RT-qPCR. Primers of RT-qPCR are listed in Table S4. RT-qPCR analysis was performed using iTaq SYBR Green on an Applied Biosystems ABI Vii7 Sequence Detection System using standard cycling conditions, and mRNA expression values were quantified with corresponding standard curves and normalized to housekeeping genes GAPDH.

2.10 | Immunoblot analysis

Cells were collected and proteins were extracted using NP-40 lysis buffer with proteinase inhibitors and quantified using a BCA protein assay kit. Equal amounts of protein were separated by 10% or 12% SDS-PAGE and transferred onto $0.22 \mu\text{m}$ PVDF membranes. The membranes were blocked and incubated with the primary antibodies at 4°C overnight, and then incubated with HRP-conjugated primary antibodies at room temperature for 40 min. The protein bands were visualized by X-ray film using a freshly made electrochemiluminescence reagent.

2.11 | Bioinformatic analysis

The NB tumor RNA sequencing and clinical data were profiled via the SEQC project and downloaded from the GEO website (<https://www.ncbi.nlm.nih.gov/geo/>), including the GSE49711 dataset. Clinical data from patients with NB were used to determine the expression level of 20 candidate/known oncogenes with or without MYCN amplification and the difference in overall survival between NB patients with low or high expression of these genes. Among these genes, the difference between *TAF1D* mRNA levels among INSS stages and between non-high-risk versus high-risk patients

was further analyzed. Additionally, The TAF1D expression levels in MYCN-amplified and MYCN-non-amplified NB as well as survival analysis in Kocak-649 and Westermann-144 neuroblastoma datasets were analyzed via the Genomics Analysis and Visualization Platform (R2; <http://r2.amc.nl>).

2.12 | Statistical analysis

GraphPad Prism version 8 software program (GraphPad Software) was used to analyze the mRNA levels and other quantification data. JMP pro16 (SAS Institute) was used to analyze Depmap datasets. Most of the data are presented as the mean \pm SD. Differences between groups were analyzed using the Student's *t*-test or two-way ANOVA. The *p*-values of gene mRNA levels among MYCN status and risk level were calculated using a linear model with the R package *limma*, and the *p*-values of INSS stages were calculate by one-way ANOVA. The log-rank test was used to determine the *p*-value in the overall survival analysis. Statistical significance in this study was set at *p* < 0.05.

3 | RESULTS

3.1 | Targeted siRNA screen identified TAF1D as an oncogenic driver in MYCN-amplified HR-NB cells

To identify new essential genes in MYCN-amplified HR-NB, we analyzed a dataset of 498 well annotated cases of NB (GSE49711, SEQC-498)¹⁹ and selected genes that were highly expressed in MYCN-amplified HR-NB (\log_2 FC MYCN-amplified vs MYCN-non-amplified > 0.8, *p* < 0.05) as well as negatively correlated with survival (*p* < 0.05). After excluding genes with well defined functions in NB, we analyzed the remaining genes using a protein-protein interaction network and function prediction databases (i.e., STRING, IntAct, GENECARD), which finally prioritized 19 genes with possible roles in NB (Figure 1A, Figure S1). Next, we designed a small-interfering RNA (siRNA) library targeting these 19 candidate genes as well as targeting *GPC2*, which has an established role in NB, as a positive control²⁰ (Figure 1A). We transfected the MYCN-amplified NB cell line, SK-N-BE(2), with one of the 20 pools of siRNAs and with *Luciferase*-targeting siRNA as a negative control.²¹ Then, cells

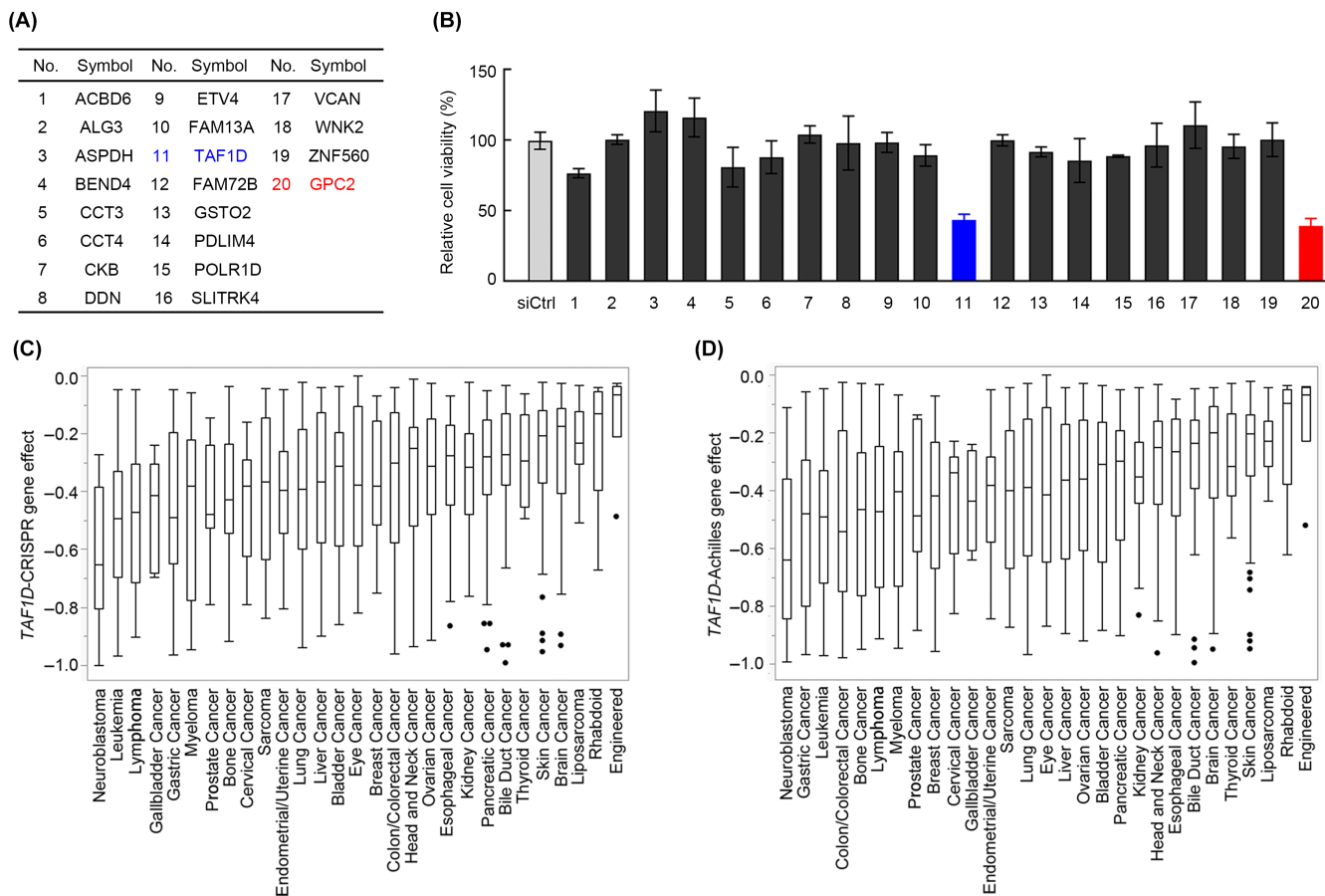


FIGURE 1 Identification of TAF1D as a potential oncogene in MYCN-amplified NB. (A) In total, 20 candidate/known oncoproteins in neuroblastoma. (B) Small-scale RNAi screen using a library targeting potential oncoproteins in neuroblastoma. (C) *TAF1D* gene_effect analysis of tumor cells in CRISPR_gene_effect Depmap dataset. (D) *TAF1D* gene_effect analysis of tumor cells in Achilles_gene_effect Depmap dataset.

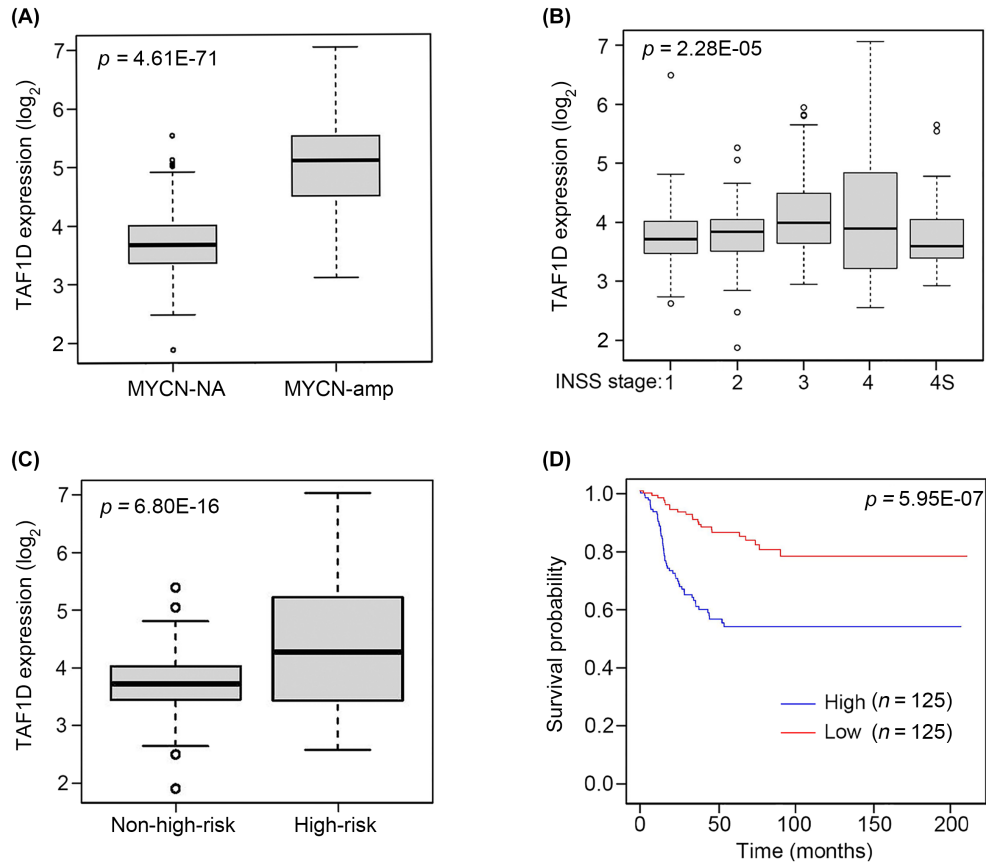


FIGURE 2 *TAF1D* expression is associated with clinical characteristics of NB. (A–C) *TAF1D* expression in samples stratified according to MYCN status, INSS stage, and risk group; data were obtained from the GSE49711 dataset (SEQC-498). (D) Kaplan–Meier analysis of overall survival in patients with NB with high or low expression of *TAF1D*; Cutoff mode: quartiles, high expression of *TAF1D* group means the highest quartile NB cases ($n = 125$) and low expression of *TAF1D* group means the lowest quartile NB cases ($n = 125$). amp: amplification; NA: non-amplification.

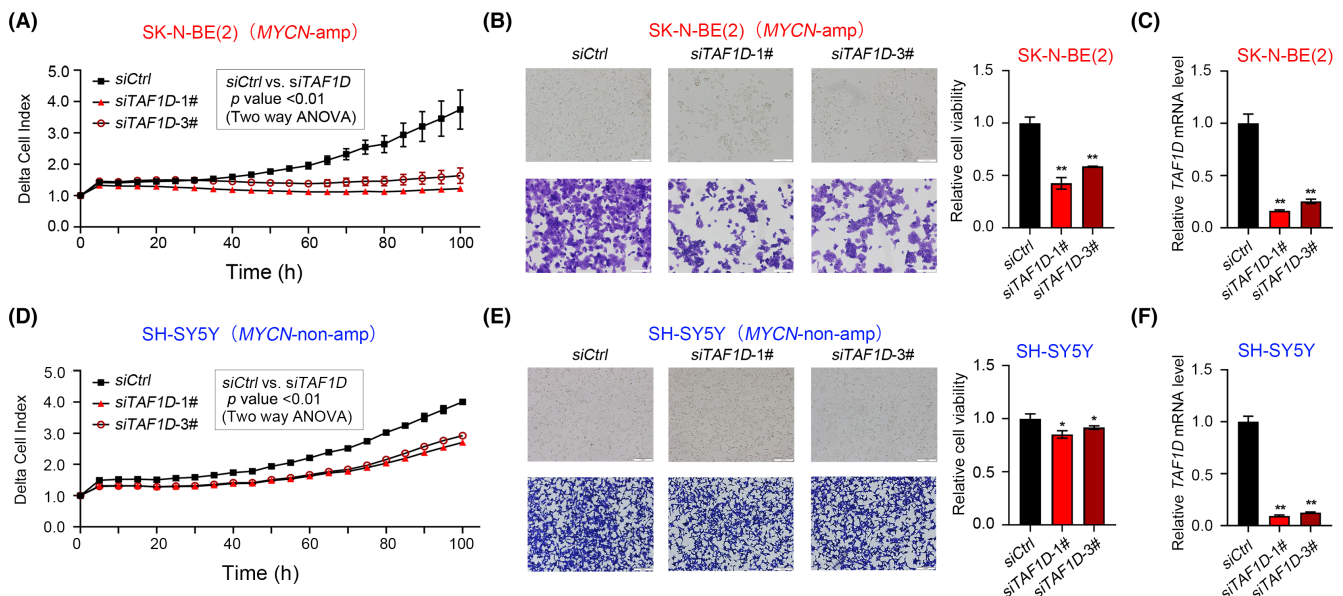


FIGURE 3 siRNA-mediated knockdown of *TAF1D* inhibits MYCN-amplified NB cell growth more effectively. (A, D) RTCA monitoring of MYCN-amplified SK-N-BE(2) cells (A) or MYCN-non-amplified SH-SY5Y cells (D). (B, E) Representative images and quantification of crystal violet staining of SK-N-BE(2) (B) or SH-SY5Y cells (E) 72 h after transfection. (C, F) mRNA expression levels of *TAF1D* in control and siRNA-*TAF1D* groups in SK-N-BE(2) (C) or SH-SY5Y cells (F). ** $p < 0.01$, * $p < 0.05$.

were analyzed using crystal violet staining to identify proteins required for cell viability. As expected, GPC2 knockdown significantly reduced cell viability, and we also observed that the knockdown of *TAF1D* markedly reduced the viability of *MYCN*-amplified NB cells (Figure 1B). Consequently, we queried the Avana library in the Depmap datasets, which contains genome-scale CRISPR/Cas9 loss-of-function screening data from a collection of 987 human cancer cell lines from 29 tumor types,^{22,23} and we found that the gene effect score of *TAF1D* was lowest in NB compared with all other tumor types, indicating that the highest toxicity was observed following *TAF1D* knockout in NB than other tumor types (Figure 1C). Further, in the Achilles-gene-effect dataset screening the effect of gene deficiency in 926 human cancer cell lines from 29 tumor types in the Depmap datasets,^{24,25} *TAF1D* deficiency was most toxic in NB tumors compared with all others (Figure 1D). Collectively, our results implicated *TAF1D* as a newly discovered essential gene in NB.

3.2 | *TAF1D* is associated with disease progression and poor clinical outcomes in patients with NB

TAF1D is a transcriptional regulator,¹⁵ but whether it has any role in NB carcinogenesis is unknown. To assess the contribution of *TAF1D* to NB pathogenesis, we further analyzed the relationship between

TAF1D expression level and clinical outcomes in a 498 neuroblastoma cohort. *TAF1D* expression was higher in *MYCN*-amplified NB compared with *MYCN*-non-amplified NB (Figure 2A), and INSS stage 3 and stage 4 NBs had higher *TAF1D* expression compared with stage 1/2/4S (Figure 2B). Additionally, *TAF1D* expression was higher in HR-NB compared with non-HR-NB (Figure 2C). Finally, Kaplan–Meier analysis revealed that higher *TAF1D* expression was associated with poorer overall survival in patients with NB (Figure 2D, Figure S2C). In addition, we further analyzed the *TAF1D* expression levels and overall survival in two other neuroblastoma datasets (Kocak, $n=649$; Westermann, $n=144$) via the Genomics Analysis and Visualization Platform (R2; <http://r2.amc.nl>). Consistently, *TAF1D* expression levels were also higher in *MYCN*-amplified NB and high *TAF1D* expression was negatively associated with the survival of NB patients in these datasets (Figure S2A,B,D,E). Taken together, these observations suggest that highly expressed *TAF1D* correlated with poor clinical outcomes in patients with NB.

3.3 | *TAF1D* knockdown more potently inhibits the proliferation and colony formation in *MYCN*-amplified compared with *MYCN*-non-amplified NB cells

Because *TAF1D* expression was associated with *MYCN* amplification status and NB progression, we next investigated whether *TAF1D*

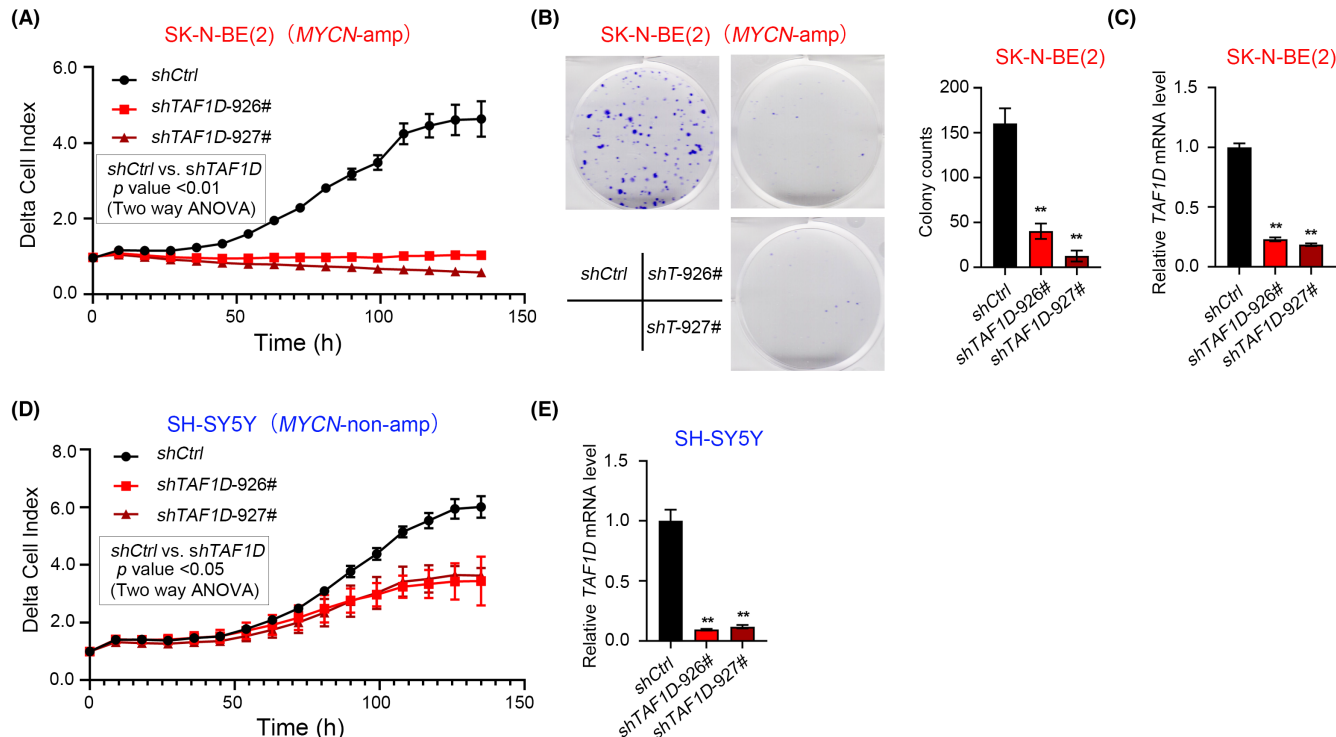


FIGURE 4 shRNA-mediated knockdown of *TAF1D* reduces the viability in *MYCN*-amplified NB cell lines more effectively. (A, D) RTCA monitoring of stable *TAF1D*-knockdown (shTAF1D-926# and shTAF1D-927#) and control group in *MYCN*-amplified SK-N-BE(2) cells (A) or *MYCN*-non-amplified SH-SY5Y cells (D). (B) Representative images and quantification of colony formation in SK-N-BE(2) cells with shRNA constructs as indicated. (C, E) *TAF1D* mRNA expression levels in SK-N-BE(2) (C) or SH-SY5Y cells (E) with *TAF1D*-targeting or control shRNA as indicated. ** $p < 0.01$.

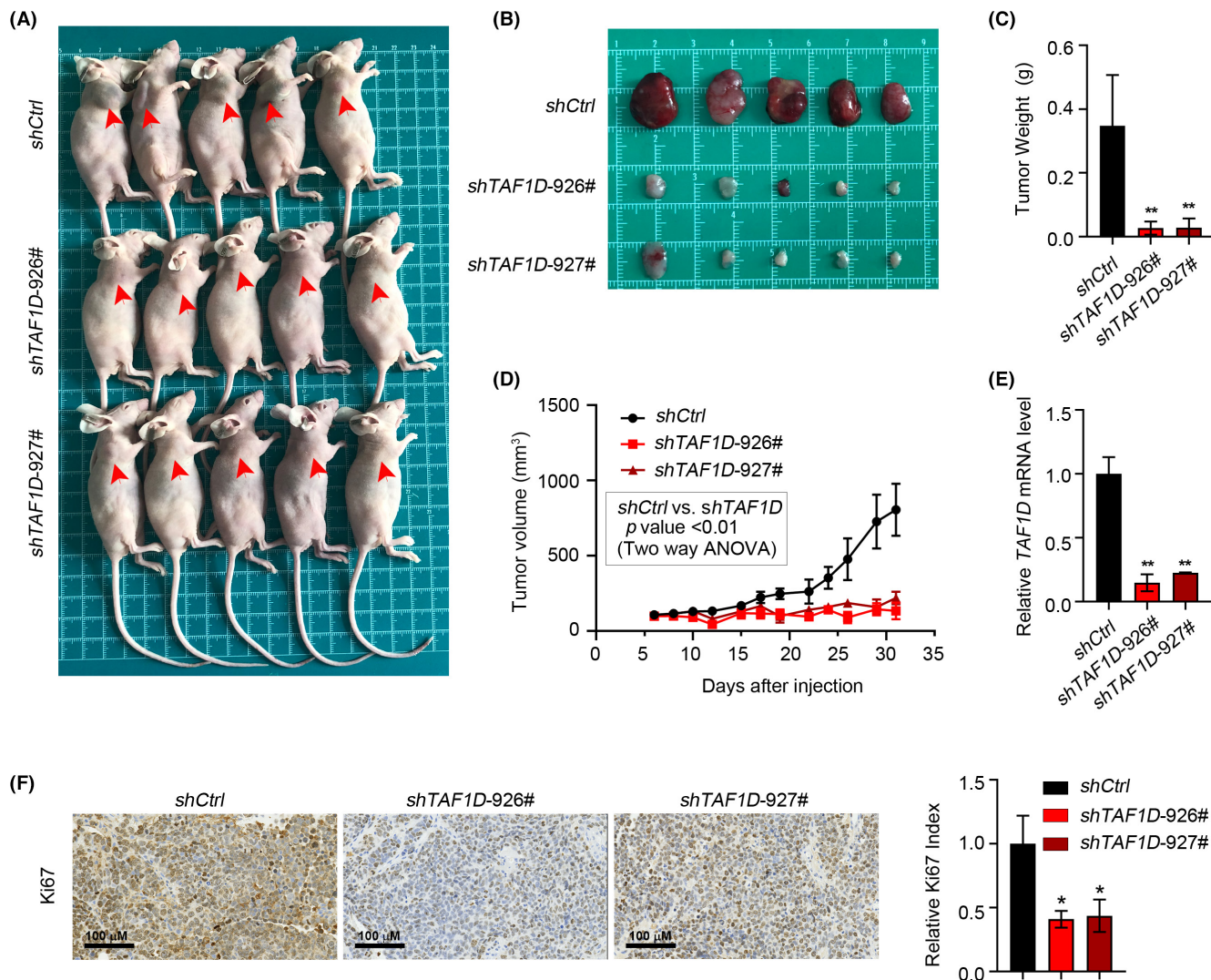


FIGURE 5 *TAF1D* knockdown inhibits growth of *MYCN*-amplified NB in vivo. (A) Images of xenograft mice. (B) Images of xenograft tumors. (C) Tumor weight. (D) Tumor volume. (E) *TAF1D* mRNA expression levels in SK-N-BE(2) xenografts with *TAF1D*-targeting or control shRNA as indicated. (F) Representative images and quantification of Ki-67 immunostaining in SK-N-BE(2) xenografts with *TAF1D*-targeting or control shRNA as indicated. Mean \pm SEM is used in Figure 5D. **p* < 0.05, ***p* < 0.01.

was required for proliferation and colony formation. We transfected the *MYCN*-amplified NB cell lines (SK-N-BE(2) and IMR32 cells)⁴ and *MYCN*-non-amplified NB cell lines (SH-SY5Y and SK-N-SH)²⁶ with two independent *TAF1D*-targeting siRNA or non-targeting control siRNA. Next, we monitored their dynamic proliferation using RTCA.²⁷ *TAF1D* knockdown decreased the delta cell index more robustly in *MYCN*-amplified NB cells compared with *MYCN*-non-amplified NB cells, indicating *TAF1D* may play a specific role in *MYCN*-amplified NB cell proliferation (Figure 3A,D). An additional assessment of cell proliferation using crystal violet staining also revealed that *TAF1D* knockdown decreased the viability of *MYCN*-amplified NB cells more significantly compared with *MYCN*-non-amplified cells (Figure 3B,E, Figure S3A,C). Efficient knockdown of *TAF1D* was confirmed by RT-qPCR in all four cell lines (Figure 3C,F, Figure S3B,D). Similar proliferation phenotypes were observed in these cell lines upon stable transfection with two independent

shRNAs named *shTAF1D-926#* and *shTAF1D-927#* validated by RT-qPCR (Figure 4A,C-E, Figure S4A,C). Consistent with these findings, colony formation assays revealed that *TAF1D*-targeting shRNA robustly reduced colony numbers compared with controls in both *MYCN*-amplified NB cells (Figure 4B, Figure S4B). Taken together, these data suggest that *TAF1D* facilitates the proliferation and colony formation of *MYCN*-amplified NB cells more effectively.

3.4 | *TAF1D* knockdown limits the growth of *MYCN*-amplified NB tumors

To explore the role of *TAF1D* in tumors, we established subcutaneous xenografts in BALB/c-nude mice using SK-N-BE(2) cells infected with *TAF1D*-targeting or control shRNA as previously described.²⁸ *TAF1D* knockdown with either validated shRNA resulted

in significantly smaller tumors compared with controls (Figure 5A–E). In agreement with our in vitro data, immunohistochemical staining showed that the proliferation marker, Ki-67,²⁹ was significantly lower in tumors from both *TAF1D*-knockdown groups compared with the control (Figure 5F). We conclude that *TAF1D* deficiency impaired in vivo tumor formation in a subcutaneous xenograft model of NB, suggesting it could be an oncogenic driver in *MYCN*-amplified NB.

3.5 | *TAF1D* knockdown impairs cell-cycle progression by transcriptionally regulating cell-cycle-related genes in *MYCN*-amplified NB cells

To investigate which pathways might be linked to the growth arrest phenotype observed in *TAF1D*-knockdown cells, we performed RNA-seq analysis on SK-N-BE(2) cells harboring two different *TAF1D* siRNA targeting (*siTAF1D-1#*, *siTAF1D-3#*) or two different negative control siRNA targeting (*siCtrl-1#*, *siCtrl-2#*) 72h after siRNAs transfection. Compared with the negative control groups, *TAF1D* knockdown significantly changed gene expression profiles (Figure 6A), with good reproducibility between the two *TAF1D*-targeting siRNAs used (Figure 6B). Kyoto Encyclopedia of Genes and Genomes (KEGG) analysis using the DAVID functional annotation tool was employed to categorize the differentially expressed genes, and the results were visualized using the R language.³⁰ Because *TAF1D* is the component of transcription factor complex that induces gene expression, we focused on genes that were downregulated by *TAF1D* knockdown for KEGG analysis, and we found that *TAF1D* knockdown decreased the expression of genes involved in various biological processes,

especially genes involved in cell-cycle progression (Figure 6C). In particular, *TAF1D* knockdown downregulated genes associated with G2/M (Figure 6D), suggesting that decreased expression of these genes may directly contribute to the observed proliferation phenotype in *TAF1D*-knockdown cells.

We next validated a subset of cell-cycle relevant genes whose expression was decreased upon *TAF1D* knockdown by RT-qPCR, including G2/M phase-related genes (e.g., *CDK1*, *ANAPC1*, and *BUB1*)^{31,32} (Figure 7A, Figure S5). As expected, these G2/M-associated genes were reduced dramatically, whereas the expression of *CDK4* and *CDK6* was barely changed by *TAF1D* knockdown (Figure 7A), consistent with the RNA-seq results. We also evaluated the protein levels of *CDK1*, *CDK4*, and *CDK6* in SK-N-BE(2) cells, and the changes in protein levels were similar to the changes in gene expression for all three genes (Figure 7B). The *CDK1* protein level was also reduced in *TAF1D*-knockdown xenograft tumors (Figure 7C).

Given that *CDK1* is the primary kinase that drives the G2/M transition to enter mitosis,³³ we next analyzed cell-cycle progression in *TAF1D*-knockdown SK-N-BE(2) cells by flow cytometry. In agreement with our RNA-seq analysis, the knockdown of *TAF1D* led to an obvious accumulation of cells in G2/M (Figure 7D). Additionally, we observed a sub-G1 fraction of cell cycle in *TAF1D*-knockdown cells 72h after siRNA transfection, indicating that *TAF1D* knockdown may induce apoptotic cell death following a sustained G2/M arrest (Figure 7D). In summary, our data support a role for *TAF1D* in cell-cycle progression and proliferation in NB cells through transcriptional regulation of cell-cycle-related genes and suggest that *TAF1D* therapeutic targeting may be an effective approach to treat *MYCN*-amplified HR-NB.

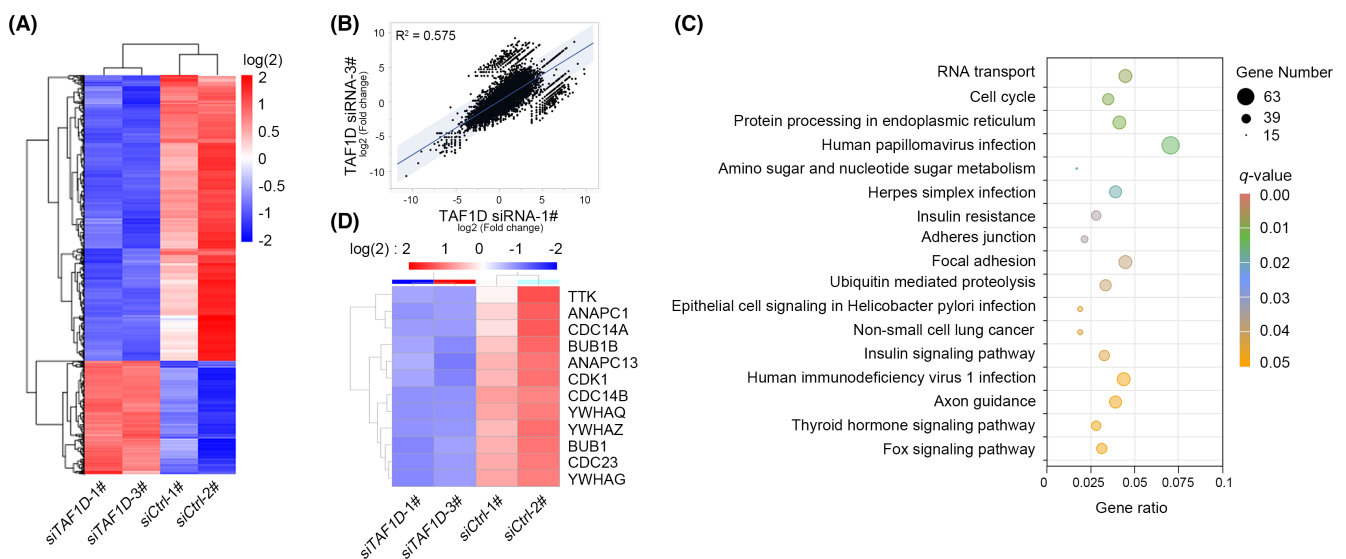


FIGURE 6 *TAF1D* knockdown reduces the expression of cell cycle-related genes. (A) Cluster heatmap of gene expression in SK-N-BE(2) cells transfected with two different *TAF1D* siRNA-targeting (*siTAF1D-1#*, *siTAF1D-3#*) or two different negative control siRNA-targeting (*siCtrl-1#*, *siCtrl-2#*) 72h after transfection. (B) Correlation plot between the fold change in gene expression in SK-N-BE(2) cells with the two independent *TAF1D*-targeting siRNAs. (C) KEGG analysis of changed genes in SK-N-BE(2) with *TAF1D*-targeting or control siRNA as indicated. (D) Heatmap of representative cell cycle genes affected by *TAF1D* knockdown in SK-N-BE(2) cells.

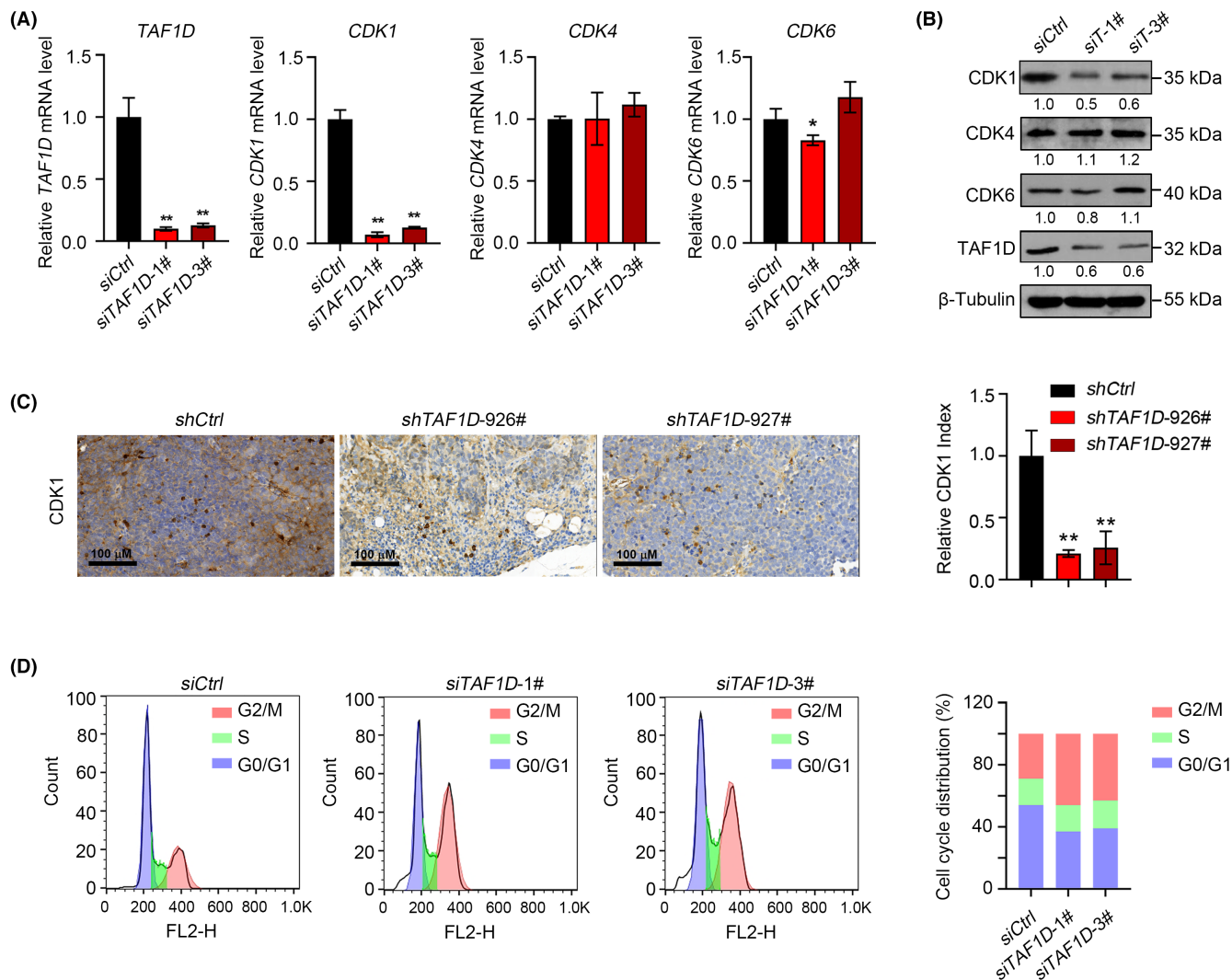


FIGURE 7 *TAF1D* knockdown induces G2/M arrest. (A, B) mRNA expression levels (A) or protein level quantification (B) of *TAF1D*, *CDK1*, *CDK4*, and *CDK6* in SK-N-BE(2) cells with *TAF1D*-targeting or control siRNA as indicated 72 h after transfection. (C) Representative images and quantification of CDK1 immunostaining in SK-N-BE(2) xenografts (Figure 5) with *TAF1D*-targeting or control shRNA as indicated. (D) Cell-cycle analysis of SK-N-BE(2) cells with *TAF1D*-targeting or control siRNA as indicated. * $p < 0.05$, ** $p < 0.01$.

4 | DISCUSSION

MYCN amplification is the most common oncogenic lesion in HR-NB.⁶ Because it is associated with poor clinical outcomes, *MYCN* amplification is used as a biomarker for risk stratification.⁵ However, owing to the lack of a druggable binding pocket, *MYCN* is not amenable to direct pharmacologic inhibition.³⁴ Therefore, exploiting the *MYCN* dependency in HR-NB requires rational drug strategies to target pathways specifically activated in *MYCN*-amplified HR-NB. To this end, we prioritized 19 genes based on high expression levels and association with poor clinical outcomes in HR-NB to test for their effect on the viability of *MYCN*-amplified HR-NB cells. We determined that *TAF1D* is required for cell viability and proliferation, colony formation, and tumor growth especially in *MYCN*-amplified HR-NB models. Furthermore, the interrogation of publicly available datasets showed that *TAF1D* was overexpressed in HR-NB and was associated with poor clinical outcomes

in patients with NB. Collectively, our results demonstrate that *TAF1D* potentiates cell proliferation and tumorigenesis in HR-NB and warrants further study as a potential therapeutic target and new biomarker for HR-NB.

We hypothesized that the role of *TAF1D* in HR-NB cell proliferation may depend on its transcriptional regulator activity. Indeed, RNA-seq analysis confirmed that *TAF1D* knockdown downregulates the expression of a set of genes involved in the cell cycle and G2/M, including *CDK1* and APC/C components (e.g., *ANAPC1* and *ANAPC13*).^{31,33} It is well known that depletion of *CDK1* induces G2/M arrest and slows cell proliferation. Consistently, we found that *TAF1D* knockdown also induced G2/M arrest, indicating that reduced *CDK1* expression in *TAF1D*-knockdown HR-NB cells may partially explain the mechanism that underlies the proliferation phenotype. Additionally, the role of *TAF1D* on the cell cycle is supported by a phosphoproteomics study that identified G2/M-specific phosphorylation sites on *TAF1D*,¹⁷ and further functional studies

of phospho-TAF1D will be important to understand whether these sites are required for the cell-cycle effects of *TAF1D*.

Aberrant cell cycle activation and proliferation are hallmarks of cancer, and anti-cell-cycle drugs are approved for some cancer indications.^{11,35} However, the adaptive responses to cell-cycle inhibitors and therapeutic index have limited the clinical success of this class of drugs so far, and additional mechanistic insights are required to identify new molecular targets as well as to stratify patients for therapies. *TAF1D* is an understudied TAF with unknown target genes.¹⁵ Our study demonstrated that *TAF1D* controls the expression of a broad array of cell-cycle-related genes, suggesting that *TAF1D* knockdown inhibits cancer cell proliferation mainly by disrupting cell-cycle progression. A deeper mechanistic understanding of how *TAF1D* regulates the expression of these cell-cycle genes will be important for future studies.

The fact that transcription factors (TFs) have traditionally been considered “undruggable” due to significant structural disorder and the lack of small-molecule binding pockets raises concern regarding the druggability of *TAF1D*. Proteolysis targeting chimera (PROTAC)-induced protein degradation is a recently developed therapeutic strategy to quench the function of “undruggable” targets³⁶; therefore, PROTAC-mediated targeting of *TAF1D* may be a promising strategy. To this end, we are screening DNA-encoded libraries (DELs),³⁷ which are massive libraries of small molecules tagged with individual DNA bar codes, to identify candidate ligands capable of binding *TAF1D* that may enable targeting with PROTACs. Based on the three essential chemical element PROTACs,³⁸ we next to construct *TAF1D*-targeting PROTACs by combining prioritized ligand candidates, a linker, and another ligand bound to an E3 ubiquitin ligase that is highly expressed in *MYCN*-amplified HR-NB to test in *MYCN*-amplified HR-NB. Additionally, mounting evidence demonstrates that nucleic acid therapeutics (i.e., chemically modified antisense oligonucleotides [ASOs] and lipid nanoparticles [LNPs])^{39,40} as well as peptide aptamers⁴¹ can be employed to validate known factors as potential anti-tumor therapeutic targets by assessing the biological consequences of their intracellular inhibition. Further studies of these strategies may help to illuminate a viable drug development strategy for targeting *TAF1D*.

In conclusion, we demonstrated that *TAF1D* fuels the proliferation of *MYCN*-amplified HR-NB cells, and we identify a novel role of *TAF1D* in regulating the cell cycle. Compared with current strategies of drugging individual cell-cycle genes, targeting *TAF1D* represents a novel therapeutic concept to inhibit cell proliferation by targeting a broad set of cell-cycle genes, which may be less susceptible to adaptive resistance mechanisms. Our findings encourage further translational studies of *TAF1D* as a prognostic biomarker and a therapeutic target for *MYCN*-amplified HR-NB.

AUTHOR CONTRIBUTIONS

Y.C. conceived and designed the project. X.Z. and S.Z. performed most of the experiments. X.G. and Y.Z. contributed to the immunohistochemistry analysis. J.L., Y.Y., et al. provided technical support. Y.G. provided critical comments and suggestions. Y.C. and X.Z.

analyzed the data and wrote the manuscript. All authors have read and approved the final manuscript.

ACKNOWLEDGMENTS

The authors thank Pro. Yanfei Gao (Chongqing Medical University, China) for the manuscript preparation.

FUNDING INFORMATION

This work was supported by the Beijing Natural Science Foundation (7212038), National Natural Science Foundation of China (82141118 and 82172849), the R&D Program of Beijing Municipal Education Commission (KM202210025010), A grant from Beijing Hospitals Authority (QML20211201), Clinical Research Special Funding Fund of Wu Jieping Medical Foundation (320.6750.2022-03-50).

CONFLICT OF INTEREST STATEMENT

The authors declare no competing interests.

ETHICS STATEMENT

Approval of the research protocol by an Institutional Reviewer Board: N/A.

Informed Consent: N/A.

Registry and the Registration No. of the study/trial: N/A.

Animal Studies: All animal experiments were performed with the approval of the Animal Experiments and Experimental Animal Welfare Committee of Capital Medical University, Beijing, China.

ORCID

Xuan Zhang  <https://orcid.org/0000-0002-1801-5855>

REFERENCES

- Ackermann S, Cartolano M, Hero B, et al. A mechanistic classification of clinical phenotypes in neuroblastoma. *Science*. 2018;362:1165-1170.
- Dong R, Yang R, Zhan Y, et al. Single-cell characterization of malignant phenotypes and developmental trajectories of adrenal Neuroblastoma. *Cancer Cell*. 2020;38:716-733.e716.
- Matthay KK, Maris JM, Schleiermacher G, et al. Neuroblastoma. *Nat Rev Dis Primers*. 2016;2:16078.
- Harenza JL, Diamond MA, Adams RN, et al. Transcriptomic profiling of 39 commonly-used neuroblastoma cell lines. *Scientific Data*. 2017;4:170033.
- Huang M, Weiss WA. Neuroblastoma and MYCN. *Cold Spring Harb Perspect Med*. 2013;3:a014415.
- Lee JW, Son MH, Cho HW, et al. Clinical significance of MYCN amplification in patients with high-risk neuroblastoma. *Pediatr Blood Cancer*. 2018;65:e27257.
- Qiu B, Matthay KK. Advancing therapy for neuroblastoma. *Nat Rev Clin Oncol*. 2022;19:515-533. doi:10.1038/s41571-022-00643-z
- Su Y, Qin H, Chen C, et al. Treatment and outcomes of 1041 pediatric patients with neuroblastoma who received multidisciplinary care in China. *Pediatric Investigation*. 2020;4:157-167.
- Park JA, Cheung NV. Targets and antibody formats for immunotherapy of Neuroblastoma. *J Clin Oncol*. 2020;38:1836-1848.
- Malumbres M, Barbacid M. Cell cycle, CDKs and cancer: a changing paradigm. *Nat Rev Cancer*. 2009;9:153-166.
- Matthews HK, Bertoli C, de Bruin RAM. Cell cycle control in cancer. *Nat Rev Mol Cell Biol*. 2022;23:74-88.

12. Ando K, Nakagawara A. Acceleration or brakes: which is rational for cell cycle-targeting Neuroblastoma therapy? *Biomolecules*. 2021;11:750.
13. Qi Y, Ding L, Zhang S, et al. A plant immune protein enables broad antitumor response by rescuing microRNA deficiency. *Cell*. 2022;185:1888-1904.e1824.
14. Bendris N, Lemmers B, Blanchard JM. Cell cycle, cytoskeleton dynamics and beyond: the many functions of cyclins and CDK inhibitors. *Cell Cycle*. 2015;14:1786-1798.
15. Gorski JJ, Pathak S, Panov K, et al. A novel TBP-associated factor of SL1 functions in RNA polymerase I transcription. *EMBO J*. 2007;26:1560-1568.
16. Cramer P. Organization and regulation of gene transcription. *Nature*. 2019;573:45-54.
17. Pijnappel WP, Kolkman A, Baltissen MP, Heck AJ, Timmers HM. Quantitative mass spectrometry of TATA binding protein-containing complexes and subunit phosphorylations during the cell cycle. *Proteome Sci*. 2009;7:46.
18. Sahu D, Hsu CL, Lin CC, et al. Co-expression analysis identifies long noncoding RNA SNHG1 as a novel predictor for event-free survival in neuroblastoma. *Oncotarget*. 2016;7:58022-58037.
19. Xu J, Gong B, Wu L, et al. Comprehensive assessments of RNA-seq by the SEQC consortium: FDA-led efforts advance precision medicine. *Pharmaceutics*. 2016;8:8.
20. Bosse KR, Raman P, Zhu Z, et al. Identification of GPC2 as an Oncoprotein and candidate immunotherapeutic target in high-risk Neuroblastoma. *Cancer Cell*. 2017;32:295-309.e212.
21. Wu M, Chang Y, Hu H, et al. LUBAC controls chromosome alignment by targeting CENP-E to attached kinetochores. *Nat Commun*. 2019;10:273.
22. Meyers RM, Bryan JG, McFarland JM, et al. Computational correction of copy number effect improves specificity of CRISPR-Cas9 essentiality screens in cancer cells. *Nat Genet*. 2017;49:1779-1784.
23. Pacini C, Dempster JM, Boyle I, et al. Integrated cross-study datasets of genetic dependencies in cancer. *Nat Commun*. 2021;12:1661.
24. Sheffer M, Lowry E, Beelen N, et al. Genome-scale screens identify factors regulating tumor cell responses to natural killer cells. *Nat Genet*. 2021;53:1196-1206.
25. Ito T, Young MJ, Li R, et al. Paralog knockout profiling identifies DUSP4 and DUSP6 as a digenic dependence in MAPK pathway-driven cancers. *Nat Genet*. 2021;53:1664-1672.
26. Poon E, Liang T, Jamin Y, et al. Orally bioavailable CDK9/2 inhibitor shows mechanism-based therapeutic potential in MYCN-driven neuroblastoma. *J Clin Invest*. 2020;130:5875-5892.
27. Yan G, Du Q, Wei X, et al. Application of real-time cell electronic analysis system in modern pharmaceutical evaluation and analysis. *Molecules (Basel, Switzerland)*. 2018;23:3280.
28. Álvarez-León W, Mendieta I, Delgado-González E, Anguiano B, Aceves C. Molecular iodine/cyclophosphamide synergism on Chemoresistant Neuroblastoma models. *Int J Mol Sci*. 2021;22:8936.
29. Urruticochea A, Smith IE, Dowsett M. Proliferation marker Ki-67 in early breast cancer. *J Clin Oncol*. 2005;23:7212-7220.
30. Lian Y, Wang Q, Mu J, et al. Network pharmacology assessment of Qingkailing injection treatment of cholestatic hepatitis. *J Tradit Chin Med*. 2021;41:167-180.
31. Schrock MS, Stromberg BR, Scarberry L, Summers MK. APC/C ubiquitin ligase: functions and mechanisms in tumorigenesis. *Semin Cancer Biol*. 2020;67:80-91.
32. Elowe S, Bolanos-Garcia VM. The spindle checkpoint proteins BUB1 and BUBR1: (SLiM) ming down to the basics. *Trends Biochem Sci*. 2022;47:352-366.
33. Xie B, Wang S, Jiang N, Li JJ. Cyclin B1/CDK1-regulated mitochondrial bioenergetics in cell cycle progression and tumor resistance. *Cancer Lett*. 2019;443:56-66.
34. Wolpaw AJ, Bayliss R, Büchel G, et al. Drugging the "Undruggable" MYCN oncogenic transcription factor: overcoming previous obstacles to impact childhood cancers. *Cancer Res*. 2021;81:1627-1632.
35. Suski JM, Braun M, Strmiska V, Sicinski P. Targeting cell-cycle machinery in cancer. *Cancer Cell*. 2021;39:759-778.
36. Henley MJ, Koehler AN. Advances in targeting 'undruggable' transcription factors with small molecules. *Nat Rev Drug Discov*. 2021;20:669-688.
37. Goodnow RA Jr, Dumelin CE, Keefe AD. DNA-encoded chemistry: enabling the deeper sampling of chemical space. *Nat Rev Drug Discov*. 2017;16:131-147.
38. Schapira M, Calabrese MF, Bullock AN, Crews CM. Targeted protein degradation: expanding the toolbox. *Nat Rev Drug Discov*. 2019;18:949-963.
39. Mondala PK, Vora AA, Zhou T, et al. Selective antisense oligonucleotide inhibition of human IRF4 prevents malignant myeloma regeneration via cell cycle disruption. *Cell Stem Cell*. 2021;28:623-636.e629.
40. Kumthekar P, Ko CH, Paunesku T, et al. A first-in-human phase 0 clinical study of RNA interference-based spherical nucleic acids in patients with recurrent glioblastoma. *Sci Transl Med*. 2021;13:eabb3945.
41. Liu K, Xie F, Zhao T, et al. Targeting SOX2 protein with peptide Aptamers for therapeutic gains against esophageal squamous cell carcinoma. *Mol Ther*. 2020;28:901-913.

SUPPORTING INFORMATION

Additional supporting information can be found online in the Supporting Information section at the end of this article.

How to cite this article: Zhang X, Zhan S, Guan X, et al. TAF1D promotes proliferation by transcriptionally activating G2/M phase-related genes in MYCN-amplified neuroblastoma. *Cancer Sci*. 2023;114:2860-2870. doi:[10.1111/cas.15815](https://doi.org/10.1111/cas.15815)